International Journal of Fracture Fatigue and Wear, Volume 2

Proceedings of the 3rd International Conference on
Fracture Fatigue and Wear, pp. 148-154, 2014

BUCKLING OF FUNCTIONALLY GRADED CARBON NANOTUBE-FIBER REINFORCED PLATES UNDER MECHANICAL LOADS

B. Sobhani Aragh and M. Abdel wahab

Department of Mechanical Construction and Production, Faculty of Engineering and Architecture, Ghent University, Belgium

Abstract: Based on first-order shear deformation (FSDT), the mechanical buckling of a functionally graded nanocomposite rectangular plate reinforced by aligned and straight single-walled carbon nanotubes (SWCNTs) subjected to uniaxial and biaxial in-plane loadings is investigated. The material properties of the nanocomposite plate are assumed to be graded in the thickness direction and vary continuously and smoothly according to two types of the symmetric carbon nanotubes volume fraction profiles. The equilibrium and stability equations are derived using the Mindlin plate theory considering the FSDT effect and variational approach. A numerical study is performed to investigate the influences of the different types of compressive in-plane loadings, CNTs volume fractions, various types of CNTs volume fraction profiles, geometrical parameters and different types of estimation of effective material properties on the critical mechanical buckling load of functionally graded nanocomposite plates.

Keywords: functionally graded materials; mechanical buckling; first-order shear deformation; nanocomposite

1 INTRODUCTION

Functionally Graded Materials (FGMs) which are advanced multiphase composites and are engineered to have a smooth spatial variation of material constituents have attracted considerable attention recent years [1]. In most recent literature regarding FGM structures [2-3], the material properties are assumed having a smooth variation usually in one direction. In traditional nanocomposites, the resulting mechanical, thermal, or physical properties do not vary spatially at the macroscopic level since nanotubes distribute either uniformly or randomly in the composites. On the other hand, mechanical properties of nanotube-reinforced composites will deteriorate if the volume fraction of nanotubes arises beyond certain limit. Therefore, In the modelling of carbon nanotubes-reinforced composites (CNTRCs) the concept of FGM might be incorporated to effectively make use of the nanotubes. According to a comprehensive survey of literature, the authors found that there are few research studies on the mechanical behaviour of functionally graded carbon nonotube-reinforced composite (FGM-CNTRC) structures. Shen [4] studied the nonlinear bending of reinforced composite plate by SWCN under the sinusoidal loading in thermal environment. The results obtained indicated that the effect of FG distribution of CNTs causes increase in the moment and stress. Also Shen [5] investigated the thermal buckling of composite plate reinforced by CNT (FG distribution). The obtained results of the paper shown that the FG distribution of CNTs causes critical buckling temperature to be higher than the UD distribution of CNTs. Shen and Zhu [6] investigated the buckling and post-buckling of nanocomposite plates with functionally graded nanotube reinforcements subjected to uniaxial compression in thermal environments. The effective material properties of the nanocomposite plates were derived by the use of extended rule of mixture. They found that the linear functionally graded nano-reinforcement has a quantitative effect on the uniaxial buckling load as well as post-buckling strength of the plates.

The main objective of the present work is to investigate the buckling behaviour of the functionally graded nanocomposite rectangular plates reinforced by straight, single-walled CNTs subjected to uniaxial and biaxial in-plane loadings. The material properties of the nanocomposite plate are assumed to be graded in the thickness direction and vary continuously and smoothly according to two types of the symmetric carbon nanotubes volume fraction profiles. The equilibrium and stability equations are derived using the Mindlin plate theory considering the first-order shear deformation (FSDT) effect and variational approach. Resulting equations are employed to obtain the closed-form solution for the critical buckling load for each loading case. A detailed parametric study is carried out to investigate the influences of the different types of

compressive in-plane loadings, CNTs volume fractions, various types of CNTs volume fraction profiles, geometrical parameters and different types of estimation of effective material properties on the critical mechanical buckling load of functionally graded nanocomposite plates.

2 THEORETICAL FORMULATION

As shown in Fig. 1, a polymer rectangular plate with the length of *a*, width of *b* and the thickness of *t* reinforced by SWCNTs, graded distribution in the thickness direction, is assumed. It is also assumed that the mentioned nanocomposite plate is being influenced by plane forces N_x and N_y, which are in x and y direction respectively.

2.1 Mathematical modelling of FGM-CNTRC

In this paper, for the first time, two types of symmetric profiles for CNTs volume fractions are configurated. As can be seen from Fig. 2, for the first type, a mid-plane symmetric graded distribution of CNT reinforcements is achieved and both top and bottom surfaces are CNT-rich referred to as Type I FG. For the second type, the distribution of CNT reinforcements is inversed and both top and bottom surfaces are CNT-poor, whereas the mid-plane surface is CNT-rich, referred to as Type II FG. We assume the CNTs volume fraction for Type I FG follows as:

$$V_{CN} = \frac{4|z|}{h} V_{CN}^{*} \tag{1}$$

In which:

$$V_{CN}^{*} = \frac{w_{CN}}{w_{CN} + (\rho_{CN}/\rho_m) - (\rho_{CN}/\rho_m) w_{CN}} \tag{2}$$

Where w_{CN} is the mass fraction of nanotube [7], and ρ_{CN} and ρ_m are the densities of CNT and matrix, respectively. The CNTs volume fraction for Type II FG follows as:

$$\mathrm{V_{CN}} = 4\left(0.5 - \frac{|z|}{h}\right) V_{CN}^{*} \tag{3}$$

Note that $V_{CN} = V_{CN}^{*}$ corresponds to the uniformly distributed CNTR plate, referred to as UD. It should be mentioned that these two FG plates and the UD plate have the same CNT mass fraction.

In this paper, for estimating effective material properties of CNTRC two different methods including extended rule of mixture [7] and Eshelby-Mori-Tanaka approach [8] have been used.

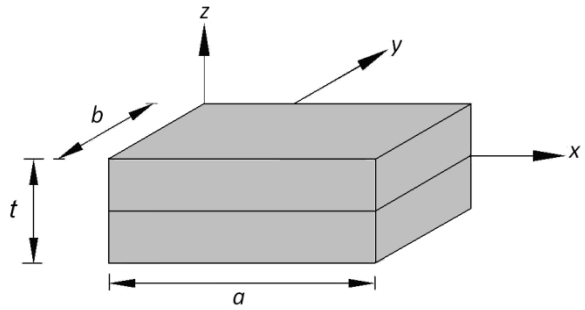

Fig. 1 Schematic of nanocomposite plate.

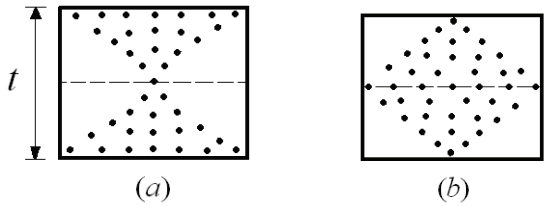

Fig. 2 Configurations of FG nanocomposite plate (Fig. (*a*): Type I FG, Fig. (*b*): Type II FG)

2.2 Equilibrium equations

According to the based on the FSDT of Mindlin [9], the displacement field of the rectangular plate is considered as

$$\begin{aligned} u(x,y,z) &= z\psi_x(x,y) \\ v(x,y,z) &= z\psi_y(x,y) \\ w(x,y,z) &= w(x,y) \end{aligned} \tag{4}$$

n which u, v and w are the displacement components in x, y and z directions respectively. ψ_x and ψ_y are also the neutral plate rotation around y and x axes, respectively.

In order to obtain the equilibrium relations, the energy method will be used. Therefore, the plate overall potential energy is written as follows:

$$V = U + \Omega \tag{5}$$

In which V is the overall potential energy, U is the elastic potential energy and Ω is work done by the external forces the relations of which are written as follows:

$$U = \frac{1}{2}\iint\int_{-t/2}^{t/2}\left(\sigma_x\varepsilon_x + \sigma_y\varepsilon_y + \sigma_z\varepsilon_z + \tau_{xy}\gamma_{xy} + \tau_{yz}\gamma_{yz} + \tau_{zx}\gamma_{zx}\right)dzdxdy \tag{6}$$

$$\Omega = \iint\left(\frac{1}{b}p_x u_{,x} + \frac{1}{a}p_y v_{,y} - p_n w\right)dxdy = \iint\left(\frac{1}{b}p_x\frac{\partial\psi_x}{\partial x} + \frac{1}{a}p_y\frac{\partial\psi_y}{\partial y} - p_n w\right)dxdy \tag{7}$$

By applying the Euler-Lagrange equations to the functional of energy, the equilibrium equations of the nanocomposite plate are obtained based on Midlin plate theory in the form below:

$$\begin{aligned} &M_{x,x} + M_{xy,y} - Q_x = 0 \\ &M_{y,y} + M_{xy,x} - Q_y = 0 \\ &\left(Q_{x,x} + Q_{y,y}\right) + \frac{\partial}{\partial x}\left(N_x\frac{\partial w}{\partial x} + N_{xy}\frac{\partial w}{\partial y}\right) + \frac{\partial}{\partial y}\left(N_{xy}\frac{\partial w}{\partial x} + N_y\frac{\partial w}{\partial y}\right) = 0 \end{aligned} \tag{8}$$

In which N_{ij} and M_{ij} are the forces and the resultant moments.

2.3 Stability equations

We give small increments to the displacement and rotation variables and examine the two adjacent configurations represented by the displacements and rotations before and after the increment, as follows:

$$\begin{aligned} \psi_x &\to \psi_{x0} + \psi_{x1} \\ \psi_y &\to \psi_{y0} + \psi_{y1} \\ w &\to w_0 + w_1 \end{aligned} \tag{9}$$

In which the subscript 0 indicates the equilibrium state and the subscript 1 expresses a minute change in the plate equilibrium condition.

By substituting the aforementioned relations into the equilibrium equations and applying the following assumptions; the linear stability equations will be obtained in the form of the Eq. (10).

1) w_0 and all its derivatives are zero.
2) The expressions conclude the N_{i0}, M_{i0} and Q_{i0} indicate the initial equilibrium condition and should be eliminated.
3) The expressions consists of multiplying the (Q_{i0}, M_{i0} and N_{i0}) in (w_{i0}, ψ_{x0} and ψ_{y0}) are negligible and should be eliminated.

$$M_{x1,x} + M_{xy1,y} - Q_{x1} = 0$$
$$M_{y1,y} + M_{xy1,x} - Q_{y1} = 0$$
$$\left(Q_{x1,x} + Q_{y1,y}\right) + \frac{\partial}{\partial x}\left(N_{x0}\frac{\partial w_1}{\partial x} + N_{xy0}\frac{\partial w_1}{\partial y}\right) + \frac{\partial}{\partial y}\left(N_{xy0}\frac{\partial w_1}{\partial x} + N_{y0}\frac{\partial w_1}{\partial y}\right) = 0 \quad (10)$$

It has been assumed that the forces are N_x and N_y in x and y directions respectively and their relation is $N_y=\gamma N_x$ (Fig. 3).By applying plate boundary condition and regarding that N_x and N_y are the plane forces per unit length applied on the plate edges one would get:

$$N_x = -\frac{p_x}{a} \qquad N_y = -\frac{p_y}{b} \quad (11)$$

$$-k\left(G_{12a} + G_{12d}\right)\left(\psi_{x1,x} + w_{1,xx} + \psi_{y1,y} + w_{1,yy}\right) - \frac{p_y}{a}w_{1,yy} - \frac{p_x}{b}w_{1,xx} = 0 \quad (12)$$

In which P_x and P_y are the total imposed forces on the plate in the direction of x and y respectively. By solving Eq. (12) the critical buckling can be obtained.

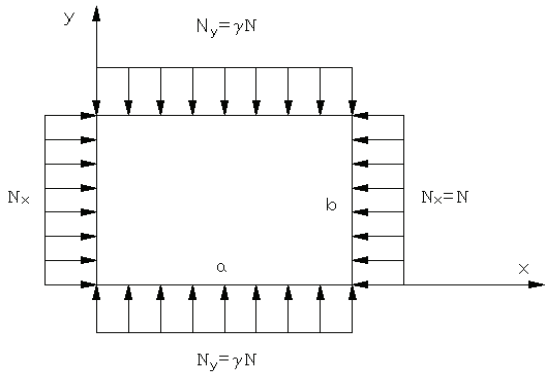

Fig. 3 Nanocomposite rectangular plate reinforced by SWCNTs under the plane forces in *x* and *y* directions ($N_x=N$, $N_y=\gamma N_x$)

3 RESULTS AND DISCUSSION

For more explanation we choose the loading of plate as follows:

1) Plane loading in the x direction.
2) Plane loading in the y direction.
3) Plane loading in the x and y directions.

For uniaxially compressed nanocomposite plate (sections 3.1 and 3.2), the extended rule of mixture is used for predicting the overall material properties and responses of the plate, while for the case of biaxial in-plane loadings (section 3.3), effective elastic moduli are computed by using Eshelby-Mori-Tanaka approach. The material properties and effective thickness of SWCNTs used for the present analysis properly are selected according to the MD simulation results of Shen [6].

3.1 Loading of plate only in *x* direction

In this section, nanocomposite rectangular plate is subjected to a uniform compressive load on edges *x*=0 and *x*=*a*. Figs. 4 shows the critical load versus the aspect ratio of *a/b* with different CNTs volume fractions and various types of CNTs volume fraction profiles. From Fig. 4, it is concluded that the critical buckling load of various types of CNTs volume fraction profiles become larger when the CNTs volume fraction increases. Another important result of Fig. 4 is that the influence of the CNTs volume fraction on the critical buckling load for different types of CNTs profiles is generally significant at high aspect ratio of *a/b*.

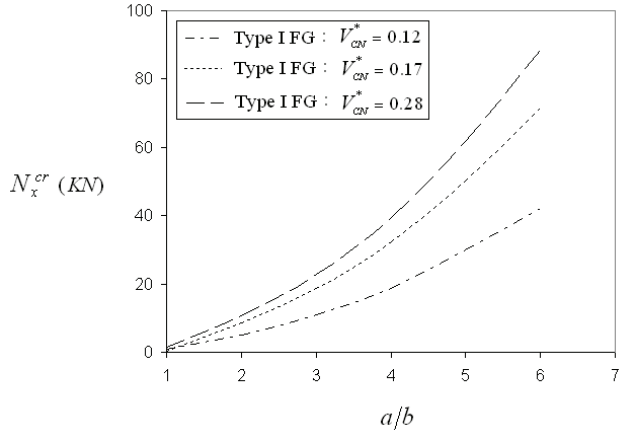

Fig. 4 Critical load $(N_x)_{cr}$ in the case of Type I FG distributed SWCNTs for various values of *a/b* (*t/b* =0.1, N_y=0)

3.2 Loading of plate only in the *y* direction

Critical buckling loads of the nanocomposite plates subjected to uniaxial in-plane loading ($N_x = 0$) are listed in Table 1 for various aspect ratio of *a/b*. It can be concluded from Table 1 that the increase of the CNTs volume fractions yields an increase in the critical buckling load. The variation of the critical buckling load versus the aspect ratio of t/b for various types of CNTs volume fraction profiles is shown in Fig. 5 for $V_{CN}^{*} = 0.12$. The results in Fig. 5 indicate that discrepancy among the various types of CNTs profiles increases with the increasing values of the aspect ratio of t/b.

Table 1 Critical buckling load N_y^{cr} (*KN*) for various types of CNTs volume fraction profiles versus *a/b* (*t*=5mm, N_x=0)

	Type I FG			UD			Type II FG		
a/b	V_{CN}^{*} =0.12	V_{CN}^{*} =0.17	V_{CN}^{*} =0.28	V_{CN}^{*} =0.12	V_{CN}^{*} =0.17	V_{CN}^{*} =0.28	V_{CN}^{*} =0.12	V_{CN}^{*} =0.17	V_{CN}^{*} =0.28
1	1.1034	1.4863	1.7067	0.9977	1.1573	1.5010	0.9011	1.0052	1.3893
2	1.2112	1.5258	1.8264	1.1143	1.2887	1.6999	1.0021	1.1362	1.6012
3	1.4396	1.8253	2.0875	1.2667	1.5014	1.9053	1.1743	1.3999	1.8111
4	1.7649	2.1002	2.3209	1.4909	1.8319	2.1876	1.5196	1.6243	1.9903
5	2.1574	2.5000	2.6999	1.8387	2.3190	2.4372	1.7784	2.1842	2.3732
6	2.5649	2.9742	3.2370	2.2989	2.6823	2.9074	2.1635	2.4987	2.8222

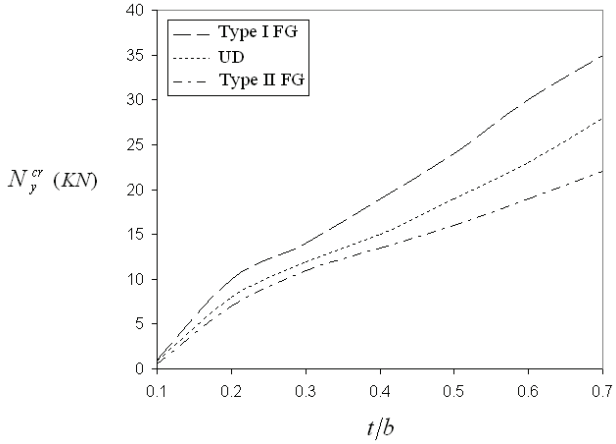

Fig. 5 Critical load $(N_y)_{cr}$ against the aspect ratio *t/b* for various types of CNTs volume fraction profiles (*a/b*=1, N_x=0, $V_{CN}^{*}=0.12$)

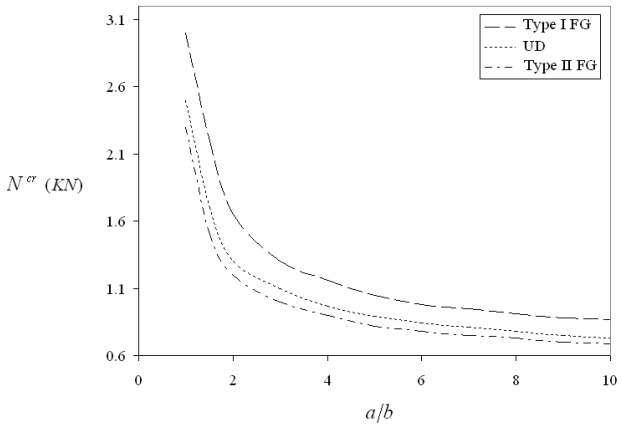

Fig. 6 Influence of different types of CNTs volume fraction profiles on critical buckling load against aspect ratio *a/b* (*t/b* =0.1, *γ*=1, $V_{CN}^{*}=0.12$)

3.3 Loading of plate in *x* and *y* directions

In this section we consider two axial loading of plate (N_x and N_y) and their relation is $N_x=\gamma N_y$. Also the material properties of the FGM nanocomposite plate are assumed to be graded in the thickness direction and estimated though the Eshelby-Mori-Tanaka approach. Influence of different types of CNTs volume fraction profiles on critical biaxial buckling load against aspect ratio *a/b* and *t/b* is presented in Figs. 6 and 7 for $V_{CN}^{*}=0.12$. It is worthy of mention that critical biaxial buckling load of the Type II FG nanocomposite plate is lower than that of one with symmetric profile (Type I FG) and close to that of the uniformly distributed CNTs. It is seen that as the aspect ratio *a/b* increases, the critical biaxial buckling load mainly decreases, while an inverse behaviour is experienced for critical uniaxial buckling load. In addition, it is found that the critical biaxial buckling load increases rapidly with increasing the aspect ratio *t/b* and then remains almost unaltered for $t/b>0.5$.

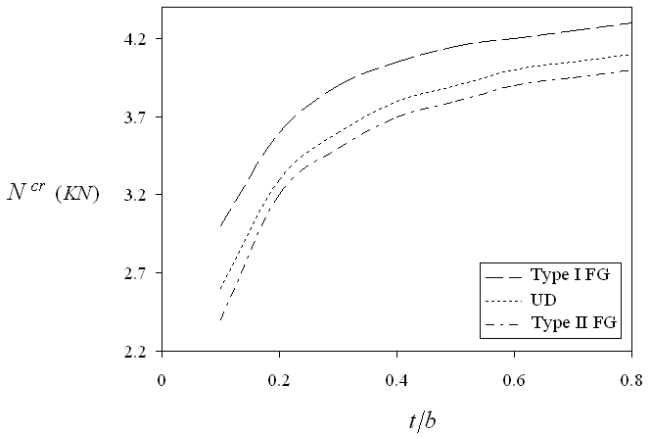

Fig. 7 Influence of different types of CNTs volume fraction profiles on critical buckling load against aspect ratio *t/b* (*a/b* =1, *γ*=1, $V_{CN}^{*} = 0.12$)

4 CONCLUSIONS

In this research work, buckling analysis of functionally graded nanocomposite rectangular plates reinforced by aligned and straight single-walled carbon subjected to uniaxial and biaxial in-plane loadings was investigated. In order to equilibrium and stability equations of the rectangular plate under in-plane load, the analysis procedure was based on the Mindlin plate theory considering the first-order shear deformation effect. Resulting equations were employed to obtain the closed-form solution for the critical buckling load for each loading case. The effective material properties of the nanocomposite plate were assumed to be graded in the thickness direction and estimated by either the Eshelby-Mori-Tanaka approach or the extended rule of mixture. Two types of the symmetric carbon nanotubes volume fraction profiles were presented in this paper. It is observed that as the aspect ratio a/b increases, the critical biaxial buckling load mainly decreases, while an inverse behaviour is experienced for critical uniaxial buckling load. Moreover, it is found that the critical biaxial buckling load increases rapidly with increasing the aspect ratio *t/b* and then remains almost unaltered for $t/b > 0.5$.

5 REFERENCES

[1] M. Koizumi, FGM activities in Japan. Compos Part B-ENG 28, 1997, 1–4.
[2] D.P.H. Hasselman, G.E. Youngblood, Enhanced Thermal Stress Resistance of Structural Ceramics with Thermal Conductivity Gradient, J. Am. Ceram. Soc. 61, 1978.
[3] Z.S. Shao, T.L. Wang, Three-dimensional solutions for the stress fields in functionally graded cylindrical panel with finite length and subjected to thermal/mechanical loads, Int. J. Solids Struct. 43, 2006, 3856–3874.
[4] H.S. Shen. Nonlinear bending of functionally graded carbon nanotube-reinforced composite plates in thermal environments. Composite Structures 2009;91:9-19.
[5] H.S. Shen, C.L. Zhang. Thermal buckling and post buckling behaviour of functionally graded carbon nanotube-reinforced composite plates. Materials and Design 2010;31:3403-11.
[6] H.S. Shen, Post-buckling of nanotube-reinforced composite cylindrical shells in thermal environments, Part II: Pressure-loaded shells. Composite Structures 93; 2011, 2496–2503.
[7] H.S. Shen and Z.H. Zhu, Buckling and Post-buckling Behaviour of Functionally Graded Nanotube-Reinforced Composite Plates in Thermal Environments, CMC 18, 2010:2;155-182.
[8] B. Sobhani Aragh, H. Hedayati, Eshelby-Mori-Tanaka approach for vibrational behaviour of continuously graded carbon nanotube-reinforced cylindrical panels. Composites: Part B 43, 2012, 1943–1954.
[9] R.D. Mindlin, Influence of rotatory inertia and shear on flexural motions of isotropic elastic plates, American Society of Mechanical Engineers Journal of Applied Mechanics:1951, 18:31-38.